Comparison of different seat-to-head transfer functions for vibrational comfort monitoring of car passengers

Daniele Carnevale[1], Ettore Pennestrì[2], Pier Paolo Valentini[2], Fabrizio Scirè Ingastone[2], Valerio Rossi[2], Massimo Cavacece[3]
[1]*Dipartimento di Informatica, Sistemi e Produzione, Università di Roma Tor Vergata, Italy*
E-mail: carneva@disp.uniroma2.it

[2]*Dipartimento di Ingegneria Meccanica, Università di Roma Tor Vergata, Italy*
E-mail: pennestri@mec.uniroma2.it , valentini@ing.uniroma2.it

[3]*Dipartmento di Ingegneria Industriale, Università di Cassino, Italy*
E-mail: cavacece@unicas.it

Keywords: Whole body vibration, ISO2631.

1 INTRODUCTION

A reliable quantitative comfort assessment for car occupants is not an easy task to achieve. Comfort is a matter of personal perception, thus a solution which may seem feasible to one could be not to another. Moreover, the complexity of the human phisiology, as well as the lack of consensus about quantitative criteria for health and vibrational comfort assessment, make this task even more difficult.

The main international standards to define the vibrational comfort of vehicle passengers through computed indices are:

- the UNI ISO-2631-1 norm [1], issued in 1985;
- the BS 6841 norm [2, 3], issued in 1987;
- the ENV 12299 norm [4], issued in 1999.

This last norm is specific for the comfort assessment of train passengers.

All these norms require the measurement of frequency-weighted accelerations at the point of entry into the body. This frequency weighting accounts for the sensitivity of the body to different frequencies vibrations. Currently turn-key systems are very expensive and used by trained personnel. This somewhat limits the gathering of experimental data, which are usually limited to short periods of time.

The principal aim of this investigation is the development of software and hardware tools for the long term and real time monitoring of whole body vibration. This require the availability of analytical models, experimental data and assembly of different hardware devices.

In our opinion the availability of low cost devices would allow:

- a long term monitoring of vibrational comfort;
- significant statistical analyses based on a measurement surveys made on a wide samples of population;

- a refinement of comfort criteria based on feedback from field users with different anthropometric features.

Bus and transport companies could be potentially interested in these devices for the monitoring of overexposure to potentially dangerous vibrations of their workers.

In order to keep the hardware to the minimum, we have chosen to implement the methodology of the ISO 2631 norm which is suitable for whole body vibration evaluation. This choice is also justified by the recent laws passed by the European Parliament. These refer specifically to this norm as a quantitative tool for assessing the limits of healthy exposure to vibrations of workers.

Purpose of this paper is to describe some of the objectives already achieved and to briefly discuss future research tasks.

The paper is organized as follows:

- the comparison of different lumped-parameter biodynamic models for the response analysis of seated human subjects;
- the coincise description of our experimental setup;
- the procedure adopted for the identification of the parameters

References [5, 6, 7] report some previous work of the auhtors on this topic.

2 DESCRIPTION OF THE MODELS

This section summarizes some of the linear models for the human response to vibration considered in this investigation. The posture of the subject is herein neglected and only the vertical motions of the lumped masses are taken into account.

The models are organized by increasing number of degrees-of-freedom. For each model are reported:

- the figure with the model depicted and the nomenclature;
- the equations of motion;
- a table with the model parameters referring to a subject of about 52-60 kg;
- a comparison between experimental and theoretical plots for the Seat-to-Head Transmissibilities (STH).

The STH transmissibility is the ratio of the maximum head acceleration $z_{\max h}$ and the maximum value $z_{\max s}$ of seat acceleration

$$STH = \left| \frac{z_{\max h}}{z_{\max s}} \right| \tag{1}$$

For its computation, it is assumed that the vehicle chassis is subjected to a vertical harmonic displacement $z_0 = Z_0 \sin \Omega t$. The STH is usually plotted as a function of the input circular frequency Ω

2.1 Coermann model

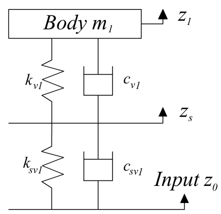

Figure 1: Schematic of Coermann model (1962)

Table 1: Coermann model biomechanical parameters

Author	Biomechanical parameters			Remarks
	Mass (kg)	Damping (Nm/s)	Stiffness (N/m)	
Coermann (1962)	$m_1 = 56.8$	$c_1 = 3840$	$k_1 = 75500$	$m_{tot} = 56.8$ Excitation: $z_0 = 5\sin\Omega t$

Equations of motion (EOM_s)

$$m_1\ddot{z}_1 + c_{v1}(\dot{z}_1 - \dot{z}_s) + k_1(z_1 - z_s) = 0 \tag{2a}$$

$$c_{sv1}(\dot{z}_s - \dot{z}_0) + k_{sv1}(z_s - z_1) = 0 \tag{2b}$$

$$STH = \left|\frac{Z_1}{Z_s}\right| = \left|\frac{k_{v1} + i\Omega c_{v1}}{k_{v1} + i\Omega c_{v1} - \Omega^2 m_1}\right| \tag{3}$$

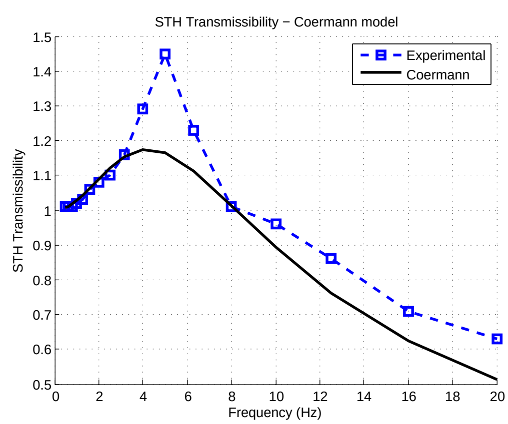

Figure 2: STH: Comparison between Coermann model and experimental data ($\varepsilon = 90.5\%$)

2.2 Wei and Griffin model

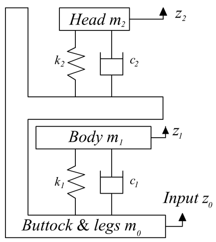

Figure 3: Schematic of Wei and Griffin model (1998)

Table 2: Wei and Griffin model biomechanical parameters

Author	Biomechanical parameters			Remarks
	Mass (kg)	Damping (Nm/s)	Stiffness (N/m)	
Wei and Griffin (1998)	$m_1 = 43.4$	$c_1 = 1485$	$k_1 = 44130$	$m_{tot} = 51.2$ Excitation: $z_0 = 5\sin\Omega t$

Equations of motion (EOM_s)

$$m_1\ddot{z}_1 + c_{v1}\left(\dot{z}_1 - \dot{z}_s\right) + k_1\left(z_1 - z_s\right) = 0 \tag{4a}$$

$$m_2\ddot{z}_2 + c_{v1}\left(\dot{z}_2 - \dot{z}_s\right) + k_2\left(z_2 - z_s\right) = 0 \tag{4b}$$

$$c_{sv1}\left(\dot{z}_s - \dot{z}_0\right) + k_{sv1}\left(z_s - z_0\right) - c_1\left(\dot{z}_1 - \dot{z}_s\right) - k_1\left(z_1 - z_s\right)$$
$$- c_2\left(\dot{z}_2 - \dot{z}_s\right) - k_2\left(z_2 - z_s\right) = 0 \tag{4c}$$

$$STH = \left|\frac{Z_2}{Z_s}\right| \tag{5}$$

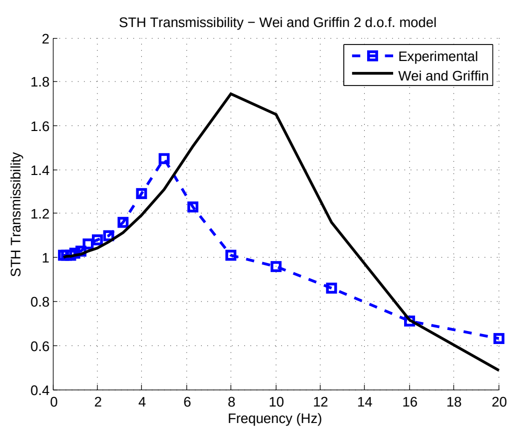

Figure 4: STH: Comparison between Wei and Griffin model and experimental data ($\varepsilon = 72.3\%$)

2.3 Suggs model

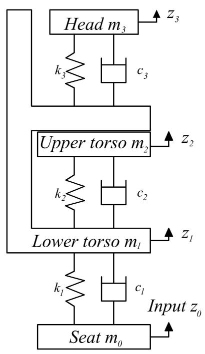

Figure 5: Schematic of Suggs model (1969)

Table 3: Suggs model biomechanical parameters

Author	Biomechanical parameters			Remarks
	Mass (kg)	Damping (Nm/s)	Stiffness (N/m)	
Suggs (1969)	$m_1 = 15.3$ $m_2 = 36.0$ $m_3 = 5.5$	$c_1 = 2806$ $c_2 = 10^4$ $c_3 = 318$	$k_1 = 40900$ $k_2 = 10^6$ $k_3 = 74300$	$m_{tot} = 56.8$ Excitation: $z_0 = 5 \sin \Omega t$

Equations of motion (EOM_s)

$$m_1\ddot{z}_1 + c_1\left(\dot{z}_1 - \dot{z}_s\right) + k_1\left(z_1 - z_s\right)$$
$$- c_2\left(\dot{z}_2 - \dot{z}_1\right) - k_2\left(z_2 - z_1\right) - c_3\left(\dot{z}_3 - \dot{z}_1\right) - k_1\left(z_3 - z_1\right) = 0 \tag{6a}$$
$$m_2\ddot{z}_2 + c_2\left(\dot{z}_2 - \dot{z}_1\right) + k_2\left(z_2 - z_1\right) = 0 \tag{6b}$$
$$m_3\ddot{z}_3 + c_3\left(\dot{z}_3 - \dot{z}_1\right) + k_3\left(z_3 - z_1\right) = 0 \tag{6c}$$
$$c_{sv1}\left(\dot{z}_s - \dot{z}_0\right) + k_{sv1}\left(z_s - z_0\right) - c_1\left(\dot{z}_1 - \dot{z}_s\right) - k_1\left(z_1 - z_s\right) = 0 \tag{6d}$$

$$STH = \left|\frac{Z_3}{Z_s}\right| \tag{7}$$

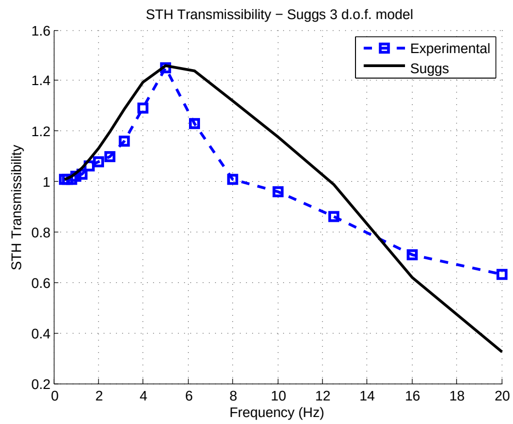

Figure 6: STH: Comparison between Suggs model and experimental data ($\varepsilon = 89.2\%$)

2.4 Wan's model

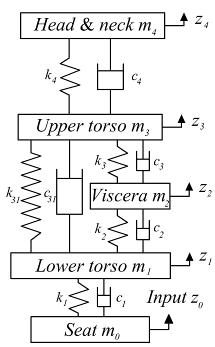

Figure 7: Schematic of Wan model (1995)

Table 4: Wan model biomechanical parameters

Author	Biomechanical parameters			Remarks
	Mass (kg)	Damping (Nm/s)	Stiffness (N/m)	
Wan (1995)	$m_1 = 36$ $m_2 = 5.5$ $m_3 = 15$ $m_4 = 4.17$	$c_1 = 2475$ $c_2 = 330$ $c_3 = 200$ $c_{31} = 909$ $c_4 = 250$	$k_1 = 49340$ $k_2 = 20000$ $k_3 = 10000$ $k_{31} = 10000$ $k_4 = 134400$	$m_{tot} = 60.67$ Excitation: $z_0 = 5\sin\Omega t$

Equations of motion (EOM_s)

$$m_1\ddot{z}_1 + c_1(\dot{z}_1 - \dot{z}_s) + k_1(z_1 - z_s) - c_2(\dot{z}_2 - \dot{z}_1) - k_2(z_2 - z_1)$$
$$- c_{31}(\dot{z}_3 - \dot{z}_1) - k_{31}(z_3 - z_1) = 0 \tag{8a}$$
$$m_2\ddot{z}_2 + c_2(\dot{z}_2 - \dot{z}_1) + k_2(z_2 - z_1) - c_3(\dot{z}_3 - \dot{z}_2) - k_3(\dot{z}_3 - \dot{z}_2) = 0 \tag{8b}$$
$$m_3\ddot{z}_3 + c_3(\dot{z}_3 - \dot{z}_2) + k_3(z_3 - z_2) + c_{31}(\dot{z}_2 - \dot{z}_1) + k_{31}(z_3 - z_1)$$
$$- c_4(\dot{z}_4 - \dot{z}_3) + k_4(z_4 - z_3) = 0 \tag{8c}$$
$$m_4\ddot{z}_4 + c_4(\dot{z}_4 - \dot{z}_3) + k_4(z_4 - z_3) = 0 \tag{8d}$$
$$c_{sv1}(\dot{z}_s - \dot{z}_0) + k_{sv1}(z_s - z_0) - c_1(\dot{z}_1 - \dot{z}_s) - k_1(z_1 - z_s) = 0 \tag{8e}$$

$$STH = \left| \frac{Z_4}{Z_s} \right| \tag{9}$$

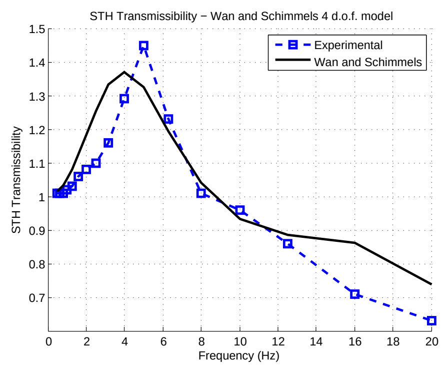

Figure 8: STH: Comparison between Wan model and experimental data ($\varepsilon = 91\%$)

3 THE EXPERIMENTAL SETUP

The experimental setup is made of two triaxial accelerometers. The first accelerometer is placed on the seat and protected by a steel lamina box and covered with synthetic rubber (neoprene). The other accelerometer, dedicated to the measurement of head acceleration, is blocked by tester teeth.

When mounting the accelerometer on the vehicle particular care must be taken to align accelerometer axes. In particular one of the axis must be directed along the direction of motion. For the remaining axes, the software computes the tilt angles ϕ and θ when the vehicle is not moving. The following transform gives the correct acceleration values

$$\left\{ \begin{array}{c} a_x \\ a_y \\ a_z \end{array} \right\} = \left[\begin{array}{ccc} -\sin\theta\cos\phi & \cos\phi & \sin\phi\cos\theta \\ \cos\theta & 0 & \sin\theta \\ -\sin\theta\cos\phi & -\sin\phi & \cos\phi\cos\theta \end{array} \right] \left\{ \begin{array}{c} a'_x \\ a'_y \\ a'_z \end{array} \right\} \tag{10}$$

The road tests have been carried out on a dedicated route. To excite the system at low frequencies, the vehicle goes on a series of road humps made with wood sticks whose section has the following dimensions 2.5 cm $\times$ 1.5 cm. The distance between two sticks is 55 cm. The length of the route with bumps is 11.5 meter.

The velocity of the vehicle is about 10 Km/h. Thus the frequency content of the input displacement is about 5 Hz. The acquisition frequency of the device is about 60Hz.

The road tests are conducted with an Audi A2 vehicle and data collected regard three male whose relevant anthropometric features are summarized in Table 5.

Table 5: Anthropometric features

Weight (kg)	Height (m)	Sex
66	1.73	Male
88	1.76	Male
78	1.80	Male

The acquisition sofware developed not only can gather and process the acceleration data to identify the model parameters, as described in the next section, but can also compute the acceleration dose according to the ISO 2631 norm.

4 MODEL IDENTIFICATION

The signals collected during the experimental campaign have been processed using a band-pass-like filter whose transfer function is depicted in Figure 9.

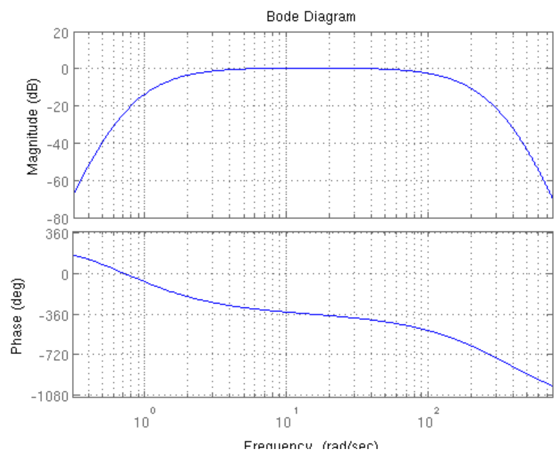

Figure 9: Signal conditioning filter: Bode diagram.

The filter magnitude is 0.039 at 0.1Hz, 1.012 at 5Hz, 0.347 at 30Hz, and 0.033 at 60Hz, respectively. The signals bias corresponding to the gravity acceleration were canceled out by the filter (the filter magnitude at 0.01Hz is about 10^{-9}).
Three experimental signals have been considered for the model identification: seat and head acceleration signals. These signals are plotted in the time domain in Figure 10.

The discrete time seat-to-head transfer function $F_{n,m}(z)$ is computed for a 30 years old person, 1.73 m tall and 66 Kg weight. The transfer function was expressed in the form

$$F_{n,m}(z) = \frac{B(z)}{A(z)}, \tag{11}$$

where $A(z) = 1 + a_1 z^{-1} + \cdots + a_n z^{-n}$, $B(z) = b_1 z^{-1} + \cdots + b_m z^{-m}$, is related to the $\mathcal{Z}$-transform of the continuous time transfer function. The unitary delay operator is z^{-1}, i. e., given a discrete time signal $x(kT)$, with sampling time T and step $k \in \mathbb{N}$, then $x(kT)z^{-1} = x((k-1)T)$.

Note that we identify the discrete time transfer function since it can be implemented in C code to evaluate on-line the norm of the passenger comfort.

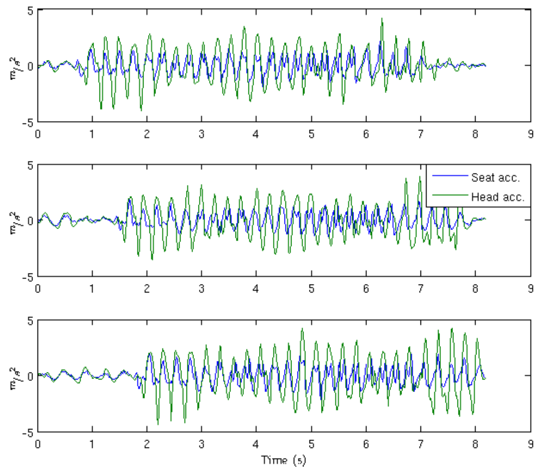

Figure 10: Experimental signals of three tests: seat and head filtered accelerations.

The Matlab function `armax` was used to estimates the coefficients of the arma (auto regressive mobile average) model expressed in the form

$$A(z)y(t) = B(z)u(t - \delta) + C(z)e(t), \tag{12}$$

where

- $u(t)$ is the seat acceleration (input);
- $y(t)$ is head acceleration (output);
- $\delta \in \mathbb{N}$ is the input delay, if any;
- $C(z) = c_0 + c_1 z^{-1} + \cdots + c_p z^{-p}$ is the regressor polynomial related to the input noise $e(t)$

An iterative search algorithm minimizes a robustified quadratic prediction error criterion. The order of the regressor polynomials $A(z)$, $B(z)$, and $C(z)$, have been chosen as $n = 8$, $m = 8$, and $p = 3$, respectively. The selected input delay is $\delta = 2$. The parameters of the function `armax` have been set to optimize the model coefficient for prediction.

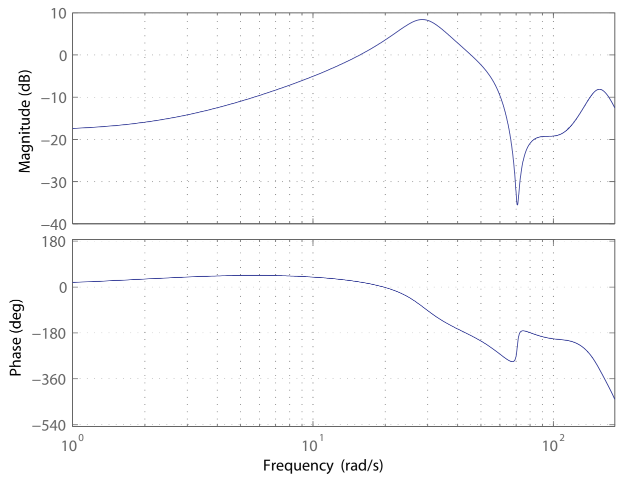

Figure 11: Estimated seat-to-head discrete time transfer function.

The tolerance has been set equal to 10^{-6} and the maximum number of iterations equal to 200. The three set of experimental data have been processed by the `armax` function to estimate an average model whose Bode diagram is shown in Figure 11 for frequency ranging from 0.16Hz (1 rad/s) to 30Hz (188.5 rad/s).

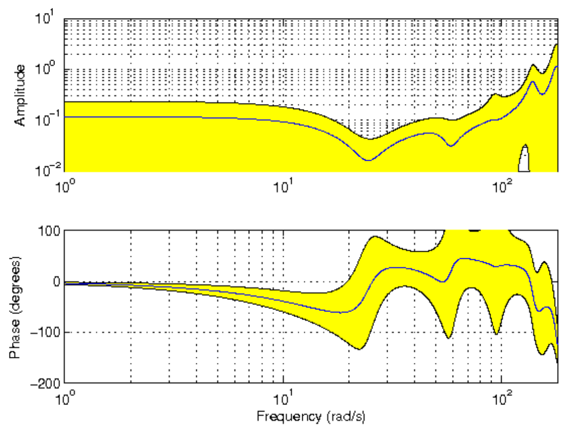

Figure 12: Prediction errors with 99% confidence intervals (yellow region).

The frequency response from the input $u(t)$ to the prediction errors, or residuals (based on a high-order FIR model), is depicted in Figure 12. The yellow marked regions corresponds to 99% confidence intervals. Since the sampling frequency is 62.5 Hz, in the Bode diagram of the identified model values greater than 180 rad/s are neglected. However, in practice, only the signals with at least one third of the sampling frequency are acceptably reconstructed. This would explain the increment of the magnitude from about 170 rad/s, which is related to aliasing-like phenomenon. This can also be sensed by the prediction errors diagram.

To show the effectiveness of the estimated model, the same set of experimental input has been processed by the identified model, obtaining the results plotted in Figure 13.

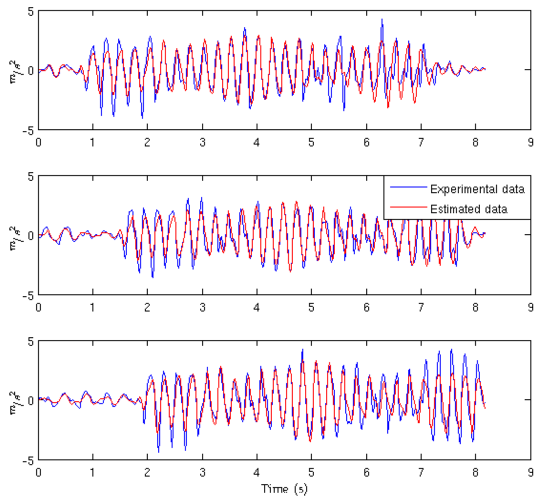

Figure 13: Identification results: output reconstruction.

5 CONCLUSIONS

In this paper are described the preliminary results of an investigation on the whole body vibration analysis. Hardware devices and software for the analysis of car passengers response to vibration have been developed. The measurements were made directly on the car.

In particular a four degrees of freedom model has been proposed and its parameters identified on the basis of collected experimental data.

References

[1] Iso 2631 Mechanical vibration and shock evaluation of human exposure to whole-body vibration.

[2] Bs6841 Guide to measurement and evaluation of human exposure to whole body mechanical vibration and repeated shock.

[3] M.J. Griffin. *Handbook of Human Vibration*. Academic Press, 1990.

[4] Env1299 Raylway applications - ride comfort for passengers- measurement and evaluation.

[5] P.P. Valentini and L. Vita. David - a multibody code to simulate a dynamic virtual dummy for vibrational comfort analysis of car occupants. In *NATO-ASI Workshop Proceedings*. 2002.

[6] E. Pennestrì, P.P. Valentini, and L. Vita. Comfort analysis of car occupant: Comparison between multibody and finite element models. *International Journal for Vehicle Systems Modeling and Testing*, 1:68–78, 2005.

[7] E. Pennestrì, R. Stefanelli, P.P. Valentini, and L. Vita. Using a virtual dummy to simulate vibration dose value for different car occupants. In *Proceedings of ASME-IDETC/CIE 2005*, 2005.